Thermodynamic and magnetic properties of the $S=1$ Heisenberg chain $Ni(C_2H_8N_2)_2Ni(CN)_4$: Experiments and theory

M. Orendáč,* A. Orendáčová, J. Černák, and A. Feher
Faculty of Science, P. J. Šafárik University, Park Angelinum 9, 04154 Košice, Slovakia

P. J. C. Signore and M. W. Meisel†
Department of Physics and the Center for Ultralow Temperature Research, University of Florida, 215 Williamson Hall, P.O. Box 118440, Gainesville, Florida 32611-8440

S. Merah and M. Verdaguer‡
Pierre and Marie Curie University, 4 Place Jussieu, 75252 Paris Cedex 05, France
(Received 14 November 1994)

Specific-heat and susceptibility studies of powdered $Ni(C_2H_8N_2)_2Ni(CN)_4$ have been performed from 50 mK to 20 K, and magnetization measurements have been conducted at 4.3 K in magnetic fields up to 6 T. The results show that $Ni(C_2H_8N_2)_2Ni(CN)_4$ is an $S=1$ antiferromagnetic Heisenberg chain with a strong planar anisotropy. The low-temperature specific-heat data show a contribution due to magnetic excitations which are interpreted within the framework of a strong coupling theory of (anti)excitons.

I. INTRODUCTION

Many theoretical and experimental studies have been devoted to the properties of one-dimensional (1D) Heisenberg magnetic systems. It has been noted that, apart from spin-wave-like excitations, large amplitude fluctuations should be considered in any attempt to describe the observed thermodynamic properties.[1] In 1983, the study of spin fluctuations in 1D systems was restimulated by Haldane's work,[2] which predicted that 1D Heisenberg antiferromagnets (HAF) with integer spin should possess an energy gap between the nonmagnetic ground state and the first excited level. Furthermore, this Haldane gap is not present in a half-integer spin HAF. The quantitative comparison of the theoretical model, which only uses nearest-neighbor exchange interactions J, with experimental results ultimately requires a more realistic Hamiltonian including single-ion anisotropy D. The numerical studies of such a system[3] revealed the presence of the Haldane phase over a range of $D/|J|$ values, namely $-0.25 \leq D/|J| \leq 1$. For an $S=1$ Heisenberg chain with $D/|J|>1$ (the so-called large D limit), another energy gap arises and generates a new singlet phase which is significantly different from one that exists for $D<|J|$. The concept of antiexcitons and excitons [hereafter referred to as (anti)excitons] as out of easy-plane fluctuations from a singlet ground state was suggested for the large D phase in a strong coupling theory.[4,5] Inelastic neutron-scattering experiments performed on the large D system of $CsFeBr_3$ (Refs. 6–8) can be interpreted[4,5] by the presence of an excitonic mode.

In this paper, we report low-temperature specific-heat, magnetic susceptibility and magnetization results of *catena*-[bis(ethylenediamine)nickel(II)-μ-cyano-dicyano-nickel(II)-μ-cyano, $Ni(C_2H_8N_2)_2Ni(CN)_4$ (hereafter abbreviated as NENC).[9] Portions of this work have been reported in preliminary form in several conference proceedings.[10,11] The analysis of the experimental data yields a consistent set of D and J parameters which support the identification of NENC as a large D HAF. More specifically, the specific-heat calculated from the excitonic dispersion relations is in a good agreement with our low-temperature data. Our results can be considered as experimental evidence for the contribution of (anti)excitons to an equilibrium thermodynamic property.

II. SYNTHESIS, CRYSTAL STRUCTURE, AND ORBITAL INTERACTIONS

Following an established procedure,[12] a $K_2Ni(CN)_4$ aqueous solution, obtained by mixing 10 ml of aqueous solution of nickel sulfate $NiSO_4 \cdot 7H_2O$ (1 mol/ℓ) and 20.5 ml of aqueous potassium cyanide KCN (2 mol/ℓ), was added to a solution obtained by mixing 10 ml of aqueous $NiSO_4$ (1 mol/ℓ) and 133 ml of an aqueous solution of 1,2-ethanediamine ($C_2H_8N_2$, abbreviated as en) (2 mol/ℓ). The mixture was stirred for 30 min, and the resulting precipitate was filtered. Single crystals ($0.2 \times 0.3 \times 0.4$ mm^3) suitable for x-ray analysis were separated from the filtrate after slow evaporation. NENC crystallizes in the monoclinic space group $P2_1/n$, $a=7.104(3)$ Å, $b=10.671(3)$ Å, $c=9.940(2)$ Å, $\beta=114.68(2)°$, $Z=2$.[9] The structure is built from neutral chains (Fig. 1) running along the c axis. The repeating unit is -[Ni(en)$_2$-NC-Ni(CN$_2$-CN]-, and two distinct nickel(II) sites are present. In the $[Ni(CN)_4]^{2-}$ anion, the nickel is in a square planar configuration, being bonded to four cyano groups through C atoms. This nickel(II) ion is diamagnetic. In the $[Ni(en)_2]^{2+}$ cation, the nickel is in a distorted octahedral configuration, where four N atoms of the two en molecules are in the basal plane ($d_{Ni\text{-}N_{en}}=2.107$ Å), while two N atoms from the cyano

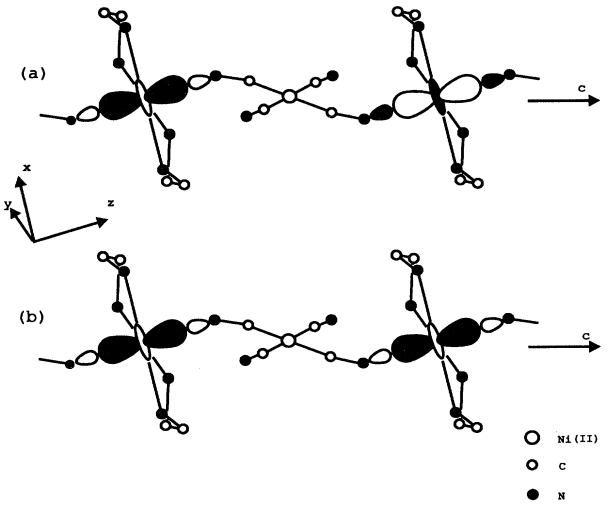

FIG. 1. A plot of the chains in NENC with the schematic representation of the weak interaction between the antibonding (a) and the nonbonding (b) z^2 magnetic orbitals along the chains. See text for a detailed discussion.

groups are in apical positions ($d_{\text{Ni-N}_{en}}=2.089$ Å). This nickel(II) ion is paramagnetic. For these paramagnetic ions, the intrachain Ni-Ni distance is 9.94 Å, whereas the shortest interchain Ni-Ni distance is 7.104 Å (along the a axis). The chain is therefore made of paramagnetic $S=1$ octahedral nickel(II) ions linked by diamagnetic square planar NC-Ni$(CN)_2$-CN units. The chains are well insulated from each other with no bonding between them. Consequently, NENC presents all the structural features required for a good quasi-1D system.

A closer look at the structure of the chains allows one to describe the unpaired electrons of the Ni(II) octahedral site by wave functions with x^2-y^2 and z^2 symmetry (e.g., in a regular octahedron), where the x and y axes are defined along the Ni-N bonds in the basal plane and the z axis is the normal to the plane, see Fig. 1. The antiferromagnetic coupling between two neighboring magnetic Ni(II) ions in the chains is expected to arise from the overlap of these orbitals in the two exchange pathways of x^2-y^2 and z^2 symmetry. It is clear from Fig. 1 that the x^2-y^2 orbitals lie in parallel basal planes and that their overlap at approximately 10 Å may be considered as negligible. The nickel(II) z^2 orbitals pointing perpendicular to the basal plane, roughly along the Ni-(NC) bonds, are more likely to overlap through the $Ni(CN)_4$ diamagnetic unit via mixing of the z^2 orbitals with the $Ni(CN)_4$ orbitals of appropriate symmetry. Such a z^2 pathway was already demonstrated in NENP (Ref. 13) through a nitrito bridge ($d_{\text{Ni-Ni}}=5.150$ Å, $J\approx -47$ K) and can be expected here with a much weaker overlap and J value. The nonbonding and antibonding combinations of z^2 orbitals are shown schematically in Fig. 1. Finally, the different chemical nature of the basal plane ligands (primary amines) and of the axial ones (cyanide ions) around the paramagnetic nickel(II) allows one to foresee some single-ion anisotropy, even if the equatorial and axial Ni-N distances are similar.

III. EXPERIMENTAL DETAILS

A. Specific heat

The specific-heat measurements of a powdered coin-shaped (15 mm in diameter and 2 mm thick) sample of 0.8 g were performed in two experimental devices. For 60 mK $< T <$ 2.5 K, the dual slope method[14] was used in an Oxford Instruments dilution refrigerator (model TLE 200). A RuO_2 thermometer (Dale RC 550 with a nominal room-temperature value of 1 kΩ) (Ref. 15) was calibrated against a commercial Lake Shore thermometer (model GR 200A-500) and served as the main thermometer. A silver wire (40 μm in diameter and 7 cm long) was used as a thermal link between the cold thermal reservoir and the platform containing the sample, the RuO_2 thermometer, and a manganin heater. The resistance of the thermometer was measured by an ac (72 Hz) resistance bridge which was connected to the controlling microcomputer via a homemade optocoupler to avoid signal interference. The experimental data were corrected for the contribution of the thermometer, the manganin heater, and the varnish (GE 7031) used to anchor the specimen to the measuring platform. This addenda contribution was measured in a separate run and was found to be 10–30% of the total heat capacity. At higher temperatures, standard adiabatic calorimetry was used in a ^{4}He cryostat equipped with a mechanical heat switch between the cold thermal reservoir and the sample cell. A 220 Ω Allen-Bradley thermometer was calibrated against the Lake Shore thermometer and served as the main thermometer in this arrangement. The overall accuracy of the dual slope data is better than 5%, while a 3% accuracy was achieved with the adiabatic technique.

B. Magnetization and susceptibility

The magnetization was measured in a ^{4}He cryostat with a homemade vibrating sample magnetometer operating at 8.2 Hz with accuracy better than 1.5%. One set of susceptibility data was obtained with a homemade superconducting quantum interference device (SQUID) magnetometer.[16] These measurements were performed on a 100.8 mg sample from 1.5 to 20 K in a static magnetic field of 0.1 mT. Another set of susceptibility data was acquired at low temperatures (50 mK to 2 K) using standard ac (217 Hz) mutual inductance coils coupled to a SQUID amplifier.[17] For these measurements, 40 mg of the 100.8 mg specimen was cooled to the lowest temperature in the presence of the earth's field before the probing ac field (≤ 15 μT) was placed on the sample. The specimen was varnished to four Cu wires (0.133 mm in diameter) which were bolted to the mixing chamber of a homemade dilution refrigerator. The temperature dependence of the signal arising from the Cu wires and the coil was measured in a separate run and was observed to be temperature independent down to about 200 mK. Below 200 mK, a small, noisy increase in the signal was detectable, and the total increase from 50 to 200 mK was approximately 3% of the change measured when the sample was present. Due to its noisy nature and small size, this background has not been subtracted from the data.

IV. RESULTS AND DISCUSSION

A. Specific heat

Heat-capacity measurements were performed in the temperature region from 60 mK to 10 K. Since NENC is a magnetic insulator, only the magnetic and the lattice contributions to the total specific heat are assumed for the present discussion. The lattice contribution was subtracted by finding the temperature region where the data may be described by the equation $C(T)=\alpha T^{-2}+\beta T^3$. The βT^3 term represents the low-temperature lattice contribution in the Debye approximation, while the αT^{-2} contribution describes high-temperature behavior of the magnetic specific heat.[18] For $5\text{K}<T<9$ K, a least-squares fit yielded $\alpha=69\pm3.5$ J K/mol, and $\beta=(3.55\pm0.15)\times10^{-3}$ J/(K^{4}mol). In order to better estimate the nonmagnetic background contributions in NENC, its diamagnetic isomorph $Zn(en)_2Ni(CN)_4$ (hereafter abbreviated as ZENC)[19] was studied from 300 mK to 10 K.[20] The subtraction of a background associated with this nonmagnetic contribution will be discussed in detail in Sec. IV C. The magnetic specific heat C_M is characterized by a round peak with the maximum value $C_{\max}=5.85\pm0.05$ J/K mol at $T_{\max}=2.4\pm0.1$ K (Fig. 2). The magnetic entropy was calculated numerically in the measured temperature region, and standard approximations were used for high and low temperatures to cover the whole temperature interval. The calculation yielded 8.68 J/K mol which is close to the theoretical value $R\ln(2S+1)=9.13$ J/K mol for an $S=1$ system. This broad maximum, together with the absence of a λ-type anomaly down to 60 mK, indicates the presence of short range correlations.

The sudden drop of C_M, observed below 1 K, suggests the existence of a gap in the energy spectrum of the spin system, and this effect is most likely associated with a magnetic anisotropy. Considering the large distances between paramagnetic Ni^{2+} ions, within or between the chains, it may be assumed that the magnetic anisotropy is due to the effect of the crystalline field. The lowest state of Ni^{2+} ions in an octahedral coordination is an orbital singlet $^3A_{2g}$. Through the combined action of spin-orbit coupling and noncubic symmetry of the crystalline field, the triply degenerate $^3A_{2g}$ level is split through the second-order perturbation with higher states. For the axial distortion of the crystalline field, the anisotropy may be described by a $D(S_z)^2$ term in the spin Hamiltonian. When the symmetry is lower (i.e., rhombic) an $E(S_x^2-S_y^2)$ term should also be included. When considering different electron density of nitrogens in en and cyano groups, it is important to stress (see Sec. II) that two kinds of ligands exist with effectively different spectrochemical nature. From this point of view, the octahedron is tetragonally elongated with a rhombic distortion due to unequal bond lengths. However, in a first approximation, the E term is neglected, and the system can be described by the Hamiltonian

$$\mathcal{H}=-2J\sum\{S_{x(i)}S_{x(i+1)}+S_{y(i)}S_{y(i+1)}+\delta S_{z(i)}S_{z(i+1)}\}+D\sum(S_{z(i)})^2 . \quad (1)$$

In Sec. IV C, the E term will be incorporated into Eq. (1), however, the physical interpretations coming from the modified Hamiltonian are not significantly different than the results presented in this Section. The specific heat of a system represented by Eq. (1) when $\delta=1$ was numerically calculated by Blöte.[21] The best agreement between the numerical predictions and the experimental data was obtained for $D/k_B\approx6$ K and $D/|J|=10$–20 (Fig. 2). The resultant $D/|J|$ ratio indicates that NENC can be considered a quantum $S=1$ chain system with a strong planar anisotropy.

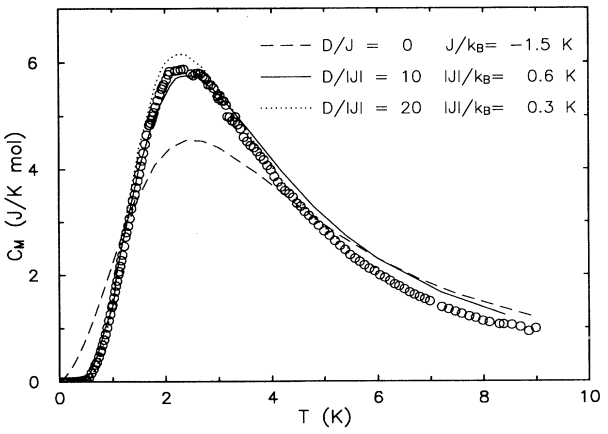

FIG. 2. The temperature dependence of the magnetic specific heat of NENC. The dashed line represents an $S=1$ HAF chain with $J/k_B=-1.5$ K, while the solid and dotted lines are for an $S=1$ HAF chain with $D/|J|=10$, $|J|/k_B=0.6$ K and $D/|J|=20$, $|J|/k_B=0.3$ K, respectively.

B. Susceptibility and magnetization

The magnetic susceptibility of a powdered sample was measured in the temperature region from 50 mK to 20 K (Fig. 1 of Ref. 11), and the field dependence of magnetization at 4.27 K was measured up to 6 T (Fig. 3). The behavior of the susceptibility data is not characterized by a round maximum typical for an isotropic HAF. To date there is no explicit expression for the temperature dependence of the susceptibility over the broad temperature range that includes the D term. Since the $D/|J|$ ratio obtained from the specific-heat results is rather large, the data above 1 K were fitted by a formula derived directly from Van Vleck equation with only D included.[18]

The best agreement between the calculated and experimental values of the susceptibility and magnetization was found for $D/k_B=6.6\pm0.2$ K, $g=2.24\pm0.01$ (Fig. 1 of Ref. 11 and Fig. 3). Alternatively, Carlin, O'Connor, and Bhatia[22] have incorporated the subcritical exchange interactions into the susceptibility within a molecular-field approximation. Applying this approach, the susceptibility data can be described by another set of constants, namely $D/k_B=6.1\pm0.2$ K, $J/k_B=-0.09\pm0.01$ K, $g=2.28\pm0.01$ (Fig. 1 of Ref. 11). For both approaches, the resultant g values are in a good agreement with $g=2.25$ reported for Ni octahedral compounds.[18] A slight change of D when J is included into the analysis

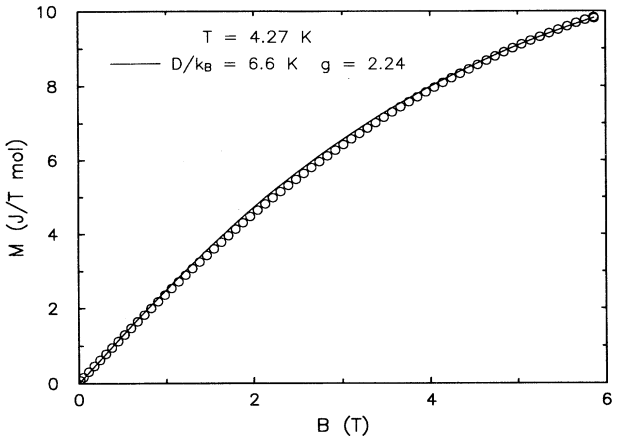

FIG. 3. Field dependence of the magnetization of NENC measured at 42.7 K. The solid curve represents an ideal paramagnet with $D/k_B=6.6$ K and $g=2.24$ as derived from fitting the susceptibility data (Fig. 1 of Ref. 11).

supports the assumption that NENC can be considered a large $D/|J|$ system. For $T<1$ K, the susceptibility deviates from the theoretical prediction and follows a Curie law. This deviation can be attributed to approximately 0.1% free paramagnetic nickel(II) ions.

C. Excitons

In the preceding subsection, the analysis of the specific-heat, susceptibility, and magnetization results have shown that NENC is an $S=1$ HAF chain with strong planar anisotropy. Furthermore, the presence of strong planar anisotropy in the compound was also confirmed by electron-paramagnetic-resonance (EPR) measurements performed on a bundle of a few small single crystals.[23]

At large D, an $S=1$ Heisenberg system with a Hamiltonian given in Eq. (1) is characterized by a unique disordered ground state in which the correlation functions decay exponentially. The first excited state is a $\Sigma S_{z(i)}=\pm 1$ doublet separated by a finite excitation gap from the ground state.[3] For the $D/|J|\rightarrow\infty$ limit, the ground-state azimuthal component of spin vanishes at every site. According to Papanicolaou and Spathis,[4,5] the lowest excited state is then constructed by exciting one spin to an azimuthal value $S_z=1$ (exciton) or $S_z=-1$ (antiexciton). The excitation energies of such states are D, $2D$, $3D$, ... (corresponding to one, two, three, or more excited spins). A finite and sufficiently small J value may be considered as a perturbation which will transform the energy levels into bands of a finite width. The low-lying bands do not overlap for a sufficiently large D/J ratio. Perturbation theory to the third order[4] was used to derive a dispersion relation for doubly degenerated (anti)excitonic mode, yielding

$$\omega_k=D[1+\omega_1/a+\omega_2/a^2+\omega_3/a^3+\cdots], \quad (2)$$

where $a=D/2J$, $\omega_1=-2\cos(k)$, $\omega_2=1+2\sin^2(k)$, and

$$\omega_3=\tfrac{1}{2}[1+8\sin^2(k)]\cos(k)-2\delta\sin^2(k).$$

In addition, the energies of two-site excitations fall into a two-body continuum. Near the Brillouin-zone boundary, some bound states smoothly emerge from the continuum. Since (anti)excitons obey Bose statistics, their specific-heat contribution will be of the form

$$C(T)=\frac{R}{\pi}\frac{d}{dT}\int_{-\pi}^{\pi}\frac{h\omega(k)}{e^{(h\omega(k)/k_BT)}-1}dk. \quad (3)$$

The comparison of the low-temperature specific-heat data with the theoretical prediction [Eq. (3)] using $D/k_B=6$ K and $D/|J|=15$ is shown in Fig. 4. As can be seen in this figure, a good quantitative agreement is obtained between the experimental data and the theoretical (anti)excitonic contribution when the D and J values from the previous specific-heat analysis (see Sec. IV A) are used. The possible contribution of two-site excitations was not taken into account since such states cannot be thermally activated in this temperature region.

A slight discrepancy between the data and the excitonic model at higher temperature occurs since, for $k_BT\gg J$, the approach of free (anti)excitons is no longer exactly valid. As can be seen in Fig. 5, there is also a discrepancy below approximately 0.4 K. The determination of the origin of this discrepancy required a more precise estimation of the lattice contribution to the specific heat. Therefore, the specific heat of the diamagnetic NENC isomorph, ZENC (see Sec. IV A), was measured from 300 mK to 10 K,[20] and a linear extrapolation was performed to lower temperatures. As can be seen in Fig. 5, the subtraction of the ZENC specific-heat data significantly improves the agreement between the (anti)excitonic contribution and the NENC specific heat below 400 mK. Furthermore, the ZENC data were compared with the results of the βT^3 fit from Sec. IV A in the interval from 300 mK to 10 K, and the deviation from the Debye law which was observed below 1 K can be attributed to the 1D structure of ZENC.[20] The remaining

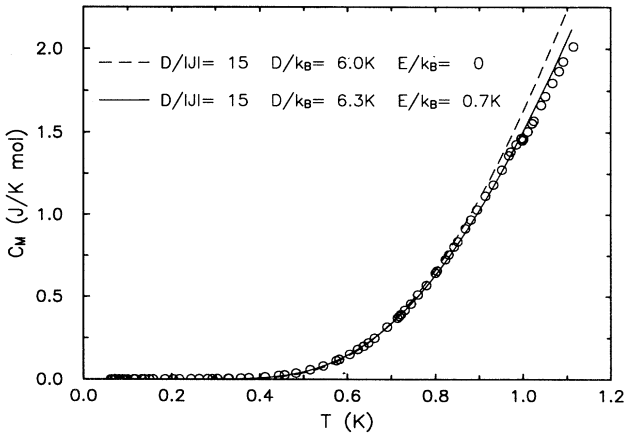

FIG. 4. Low-temperature magnetic specific heat of NENC. The data are compared to the (anti)excitonic prediction for $D/k_B=6$ K, $D/|J|=15$, $E=0$, and $D/k_B=6.3$ K, $D/|J|=15$, $E/k_B=0.7$ K, respectively.

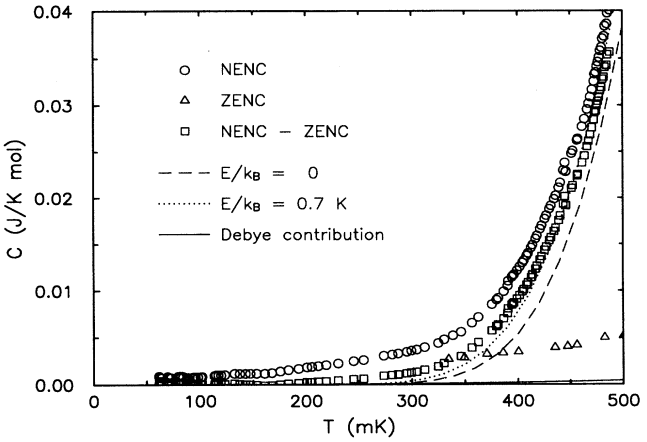

FIG. 5. Temperature dependence of the specific heat of NENC below 500 mK. The circles and squares represent the magnetic specific heat of NENC after subtracting the lattice contribution using the Debye approximation and the ZENC data, respectively. A detailed discussion of the subtraction procedure is given in the text. The ZENC data are represented by triangles. The solid line represents the Debye contribution of $(3.55\times10^{-3})\,T^3$. The dashed line represents the (anti)excitonic prediction with $D/k_B=6$ K, $D/|J|=15$, and $E=0$. The dotted curve is the result of the theoretical prediction when $D/k_B=6.3$ K, $D/|J|=15$, and $E/k_B=0.7$ K.

discrepancy might be due to the presence of a small in-plane anisotropy. Since the (anti)excitonic mode is doubly degenerate, the in-plane anisotropy represented by an $E(S_x^2-S_y^2)$ term, which is always present in real systems, causes a softening of the modes. With the $E(S_x^2-S_y^2)$ term incorporated into Eq. (1), the dispersion relations for both the excitonic and the antiexcitonic mode were recalculated.[24] The highest reduction of the mentioned discrepancy was found for $E/k_B=0.7$ K, $D/k_B=6.3$ K, and $D/J=15$ (Fig. 5). This result is consistent with the conclusion of the EPR experiment[23] that the rhombic term can be considered as a small perturbation in comparison with the planar anisotropy. It is conceivable that the powdered character of the sample might also contribute to the mentioned discrepancy, but the experimental verification of this possibility would require additional measurements to be performed on sufficiently large single crystals. Finally, we note that susceptibility data cannot be analyzed within the framework of the strong-coupling theory since the spin dynamics of a large D, $S=1$ Heisenberg chain in a magnetic field needs to be investigated theoretically.[25]

V. CONCLUSION

Our specific-heat, susceptibility, and magnetization measurements have confirmed that NENC can be considered as quantum $S=1$ HAF chain with a strong planar anisotropy. The sudden drop of the specific heat below 1 K can be ascribed to the presence of (anti)excitons predicted for large D systems by a strong-coupling theory.[4,5] The low-temperature discrepancy between the experimental data and the theoretical estimates generated by the model might be caused by the presence of a rhombic term in the Hamiltonian and/or due to the powder nature of the sample. The results suggest that NENC might be a good candidate for the inelastic neutron-scattering studies of the exciton-antiexciton bound states which, although predicted by Papanicolaou and Spathis,[4,5] have not been experimentally observed. However, sufficiently large single crystals are necessary for further studies of this system.

ACKNOWLEDGMENTS

We are very grateful to N. Papanicolaou for enlightening discussions and for recalculating the excitonic dispersion. We thank J. Kováč for the magnetization measurements and J. P. Renard and P. Veillet for the SQUID susceptibility studies performed at Orsay. The expert technical help of V. Borzenets is greatly acknowledged. Partial financial support for this work was provided by a grant from the Slovak Ministry of Education and Science (No. 1/1302/94) and the National Science Foundation (DMR-9200671). One of us (M.W.M.) acknowledges the hospitality of Northwestern University during the preparation of this manuscript.

*Electronic address: orendac@kosice.upjs.sk
†Electronic address: meisel@phys.ufl.edu
‡Electronic address: miv@ccr.jussieu.fr

[1]H. J. Mikeska and M. Steiner, Adv. Phys. **40**, 191 (1991).
[2]F. D. M. Haldane, Phys. Lett. **93A**, 464 (1983); Phys. Rev. Lett. **50**, 1153 (1983).
[3]R. Botet, R. Jullien, and M. Kolb, Phys. Rev. B **28**, 3914 (1983).
[4]N. Papanicolaou and P. Spathis, J. Phys. Condens. Matter **1**, 5555 (1989).
[5]N. Papanicolaou and P. Spathis, J. Phys. Condens. Matter **2**, 6575 (1990).
[6]B. Dorner, D. Visser, U. Steigenberger, K. Kakurai, and M. Steiner, Z. Phys. B **72**, 487 (1988); Physica B **156&157**, 263 (1989).
[7]B. Dorner, D. Visser, and M. Steiner, Z. Phys. B **81**, 75 (1990).
[8]B. Schmid, B. Dorner, D. Visser, and M. Steiner, Z. Phys. B **86**, 257 (1992).
[9]J. Černák, J. Chomič, D. Baloghová, and M. Dunaj-Jurčo, Acta Crystallogr. C **44**, 1902 (1988).
[10]M. Orendáč, A. Orendáčová, V. V. Borzenets, J. Černák, and A. Feher, Physica B **194-196**, 293 (1994).
[11]M. Orendáč, A. Orendáčová, J. Černák, A. Feher, P. J. C. Signore, M. W. Meisel, S. Merah, and M. Verdaguer, J. Magn. Magn. Mater. **140-144**, 1643 (1995).
[12]J. Černák, J. Chomič, and I. Potočňák, J. Thermal Anal. **35**, 2265 (1989).
[13]A. Meyer, A. Gleizes, J. J. Girerd, M. Verdaguer, and O.

Kahn, Inorg. Chem. **21**, 1729 (1982).
[14]S. Riegel and G. Weber, J. Phys. E **19**, 790 (1986).
[15]M. W. Meisel, G. R. Stewart, and E. D. Adams, Cryogenics **29**, 1168 (1989).
[16]P. Beauvillian, C. Chappert, and J. P. Renard, J. Phys. E **18**, 839 (1985).
[17]P. J. C. Signore, Ph.D. thesis, University of Florida, Gainesville, 1994.
[18]R. L. Carlin and A. J. van Duyneveldt, *Magnetic Properties of Transition-Metal Compounds* (Springer-Verlag, New York, 1977); R. L. Carlin, *Magnetochemistry* (Springer-Verlag, New York, 1986).
[19]J. Černák, I. Potočňák, J. Chomič, and M. Dunaj-Jurčo, Acta Crystallogr. C **46**, 1098 (1990).
[20]M. Orendáč. A. Orendáčová, J. Černák, and A. Feher (unpublished).
[21]H. W. J. Blöte, Physica **79B**, 427 (1975).
[22]R. L. Carlin, Ch. J. O'Connor, and S. N. Bhatia, J. Am. Chem. Soc. **98**, 3523 (1976).
[23]V. V. Eremenko, S. A. Zvyagin, V. V. Pishko, A. Feher, and M. Orendáč, J. Low Temp. Phys. (to be published).
[24]N. Papanicolaou has sent us the result for the (anti)exciton dispersion in the presence of a rhombic anisotropy calculated to the second order in the strong-coupling expansion. The dispersion is of the form: $\omega_{\pm}(k)=D[\omega_{\pm}(0)+\omega_{\pm}(1)/a+\omega_{\pm}(2)/a^2+\cdots]$, where $\omega_{\pm}(0)=1\pm\eta$, $\omega_{\pm}(1)=-2\cos(k)$, $\omega_{\pm}(2)=[2\sin^2(k)/(1\pm\eta)]+1/(1\mp\eta)$, and $\eta=E/D$, and $a=D/2J$.
[25]N. Papanicolaou (private communication).